PFC/JA-89-5

Variational Methods for Studying Tokamak Stability in the Presence of a Resistive Wall

Haney, S.W.; Freidberg, J.P.

January 1989

Plasma Fusion Center
Massachusetts Institute of Technology
Cambridge, MA 02139 USA

Submitted for publication in: Physics of Fluids

January 6, 1989

Variational Methods for Studying Tokamak Stability in the Presence of a Resistive Wall

S.W. Haney
Lawrence Livermore National Laboratory
University of California
Livermore, CA. 94550
USA

J.P. Freidberg
Plasma Fusion Center
Massachusetts Institute of Technology
Cambridge, MA. 02139
USA

External MHD modes stabilized by the presence of a close-fitting perfectly conducting wall become destabilized when the wall is assumed to possess finite resistivity. A simple variational principle giving an estimate for the resulting growth rate and the threshold for stability is derived in terms of quantities relating to the ideal system with and without a perfectly conducting wall. This variational principle is valid for an arbitrary three-dimensional external mode in an arbitrarily shaped plasma possessing an arbitrarily shaped, but thin, resistive wall. As an example of the utility of the method, the variational principle is used to investigate the axisymmetric ($n = 0$) stability of straight, zero pressure elliptical tokamaks with arbitrary current density profiles in the presence of a resistive wall.

I. Introduction

It is a well known from ideal MHD theory that external kink modes can be completely stabilized if a perfectly conducting wall is located sufficiently close to the plasma.[1-5] Furthermore, several authors have shown that when the perfectly conducting wall is replaced by one possessing finite resistivity, modes that were initially stable begin to grow on a timescale comparable to the resistive diffusion time associated with the wall τ_D.[6-9]

The vacuum chambers of many modern fusion devices are constructed of materials, such as stainless steel, which possess large resistivities (and correspondingly small resistive diffusion times) in order to allow quick penetration of the fields produced by external shaping and ohmic heating coils. Hence, improvements in confinement have led to situations where experimental lifetimes are potentially much greater than τ_D. This means that the estimation of growth rates for unstable modes in the presence of a resistive wall takes on great practical importance.

In this paper, we will describe a procedure, based on variational techniques, for estimating the growth rate and predicting the exact threshold condition of an arbitrary three-dimensional external mode for an arbitrarily shaped plasma in the presence of an arbitrarily shaped, but thin, resistive wall. The main contributions of the work are (1) that it yields an explicit and accurate form for the growth rate for quite general systems and (2) that this form can be evaluated solely from a knowledge of the behavior of the ideal system with perfectly conducting walls. The work thus represents a significant extension of earlier analyses.

The new procedure is derived in five parts. First, the ideal case where no wall is present is examined with the aid of the Extended Energy Principle.[10] In general, we consider systems with $\delta W < 0$ indicating instability on the ideal MHD timescale. Second, the case where a perfectly conducting wall is present is considered. Here, we assume the wall is sufficiently close to the plasma so that

δW can be made positive indicating ideal wall stabilization. Third, the effect of placing a resistive wall in place of the perfectly conducting wall is derived. This is seen to take the form of jump conditions for the tangential electric and magnetic fields across the wall. Fourth, the information gained in the previous three steps is compiled to yield a variational principle describing the dynamics of the plasma in the presence of a resistive wall. Finally, trial functions for the fields in the vacuum regions inside and outside the resistive wall are substituted into the variational principle to yield an estimate for the growth rate. The paper concludes with a discussion of non-ideal effects on resistive wall instabilities and an application of the theory to the important special case of axisymmetric ($n = 0$) tokamak stability.

II. The Ideal Case

As a point of reference, consider the stability of an arbitrary three dimensional plasma configuration with and without a perfectly conducting wall. The stability of such a system can be tested by means of the Extended Energy Principle.

A. The Wall at Infinity

When the conducting wall is moved infinitely far away the Energy Principle has the form

$$\delta W_\infty = \delta W_F + \delta W_V^{(\infty)} \tag{1}$$

where

$$\begin{aligned} \delta W_F &= \frac{1}{2}\int_{V_P}\left[\frac{|\delta\mathbf{B}|^2}{\mu_0} - \xi\cdot(\mathbf{J}\times\delta\mathbf{B}) + \Gamma p|\nabla\cdot\xi|^2 + \right. \\ &\qquad \left.(\xi\cdot\nabla p)\nabla\cdot\xi\right] dV \end{aligned} \tag{2}$$

and

$$\delta W_V^{(\infty)} = \frac{1}{2}\int_V \frac{|\delta \hat{\mathbf{B}}_\infty|^2}{\mu_0}\, dV. \tag{3}$$

Here, δW_F is the fluid energy integrated over the plasma volume and $\delta W_V^{(\infty)}$ is the vacuum energy integrated over the vacuum region surrounding the plasma. Also, it has been assumed that no surface currents flow on the plasma boundary so the surface energy $\delta W_S = 0$.

δW_F can be calculated in a straightforward manner given a trial function for the plasma displacement ξ. The vacuum energy is found by writing

$$\delta \hat{\mathbf{B}}_\infty = \nabla \times \delta \hat{\mathbf{A}}_\infty \tag{4}$$

with $\delta \hat{\mathbf{A}}_\infty$ satisfying

$$\nabla \times \nabla \times \delta \hat{\mathbf{A}}_\infty = 0. \tag{5}$$

The boundary conditions are given by

$$\delta \hat{\mathbf{A}}_\infty \Big|_\infty = 0, \tag{6}$$

$$\mathbf{e}_n \times \delta \hat{\mathbf{A}}_\infty \Big|_{S_p} = -(\mathbf{e}_n \cdot \xi)\mathbf{B} \Big|_{S_p} \tag{7}$$

where $\mathbf{e}_n$ is the outward facing unit normal vector to S_p.

Equation (7) is the linearized form of the jump condition $[\![\mathbf{e}_n \times \mathbf{E}]\!]_{S_p} = 0$. The linearized pressure balance jump condition $[\![p + B^2/2\mu_0]\!]_{S_p} = 0$ has the form

$$\mathbf{B} \cdot \nabla \times \delta \hat{\mathbf{A}}_\infty \Big|_{S_p} = \mathbf{B} \cdot \nabla \times (\xi \times \mathbf{B}) \Big|_{S_p}. \tag{8}$$

As is well known, Eq. (8) appears as a natural boundary condition in the minimization of δW. Thus, for the true minimizing solution, Eq. (8) is automatically satisfied. Conversely, for any other trial function, Eq. (8) will not be exactly satisfied. However, since the Extended Energy Principle is a variational principle, the minimization of δW (with respect to the variational parameters in the trial function) will "do as good a job as possible" in satisfying Eq. (8).

Using Eqs. (5) and (6), it is possible to cast Eq. (3) in the convenient form

$$\delta W_V^{(\infty)} = \frac{1}{2\mu_0} \int_{S_p} (\mathbf{e}_n \times \delta \hat{\mathbf{A}}_\infty) \cdot \mathbf{e}_n \times (\mathbf{e}_n \times \nabla \times \delta \hat{\mathbf{A}}_\infty)\, dS. \tag{9}$$

Wall stabilization plays an important role in systems which are unstable with the wall at infinity. Consequently, we shall hereafter consider situations where

$$\delta W_\infty < 0. \tag{10}$$

B. The Wall a Finite Distance from the Plasma

Consider now the situation where a closed, perfectly conducting wall of arbitrary shape is located a finite distance from the plasma. The surface of the wall is denoted by S_b. In addition, assume that the plasma displacement trial function ξ is identical to that used in the evaluation of δW_∞.

Under these circumstances, the potential energy can be expressed as

$$\delta W_b = \delta W_F + \delta W_V^{(b)} \tag{11}$$

where δW_F has the same value as in Eq. (1) and

$$\delta W_V^{(b)} = \frac{1}{2\mu_0} \int_{S_p} (\mathbf{e}_n \times \delta \hat{\mathbf{A}}_b) \cdot \mathbf{e}_n \times (\mathbf{e}_n \times \nabla \times \delta \hat{\mathbf{A}}_b)\, dS. \tag{12}$$

The vector potential $\delta \hat{\mathbf{A}}_b$ satisfies

$$\nabla \times \nabla \times \delta \hat{\mathbf{A}}_b = 0 \tag{13}$$

subject to the boundary conditions

$$\mathbf{e}_n \times \delta \hat{\mathbf{A}}_b \,|_{S_b} = 0, \tag{14}$$

$$\mathbf{e}_n \times \delta \hat{\mathbf{A}}_b \,|_{S_p} = -(\mathbf{e}_n \cdot \xi)\mathbf{B} \,|_{S_p}. \tag{15}$$

As might be expected, the only difference in the calculation of $\delta \hat{\mathbf{A}}_b$ compared to $\delta \hat{\mathbf{A}}_\infty$ is that the boundary condition given by Eq. (6) is replaced by Eq. (14), indicating the presence of a perfectly conducting wall.

The situations of interest for resistive wall problems are characterized by values of δW_b which are wall stabilized by a perfectly conducting wall. Hence, hereafter we shall assume that

$$\delta W_b > 0. \tag{16}$$

C. Summary of Ideal Stability

In summary, a resistive wall is expected to play a major role in the stability of external MHD modes when the system is unstable with the wall at infinity but stable with a perfectly conducting wall a finite distance from the plasma:

$$\delta W_\infty = \delta W_F + \delta W_V^{(\infty)} < 0, \tag{17}$$

$$\delta W_b = \delta W_F + \delta W_V^{(b)} > 0. \tag{18}$$

It is important to note that the values of δW_F in Eqs. (17) and (18) are identical since the same ξ has been assumed for each case.

The evaluation of the vacuum energies $\delta W_V^{(\infty)}$ and $\delta W_V^{(b)}$ is nearly identical. Both corresponding vector potentials $\delta \hat{\mathbf{A}}_\infty$, $\delta \hat{\mathbf{A}}_b$ satisfy the same equation and the same boundary condition on the surface S_p. They differ only in the outer boundary condition:

$$\delta \hat{\mathbf{A}}_\infty \big|_\infty = 0, \tag{19}$$

$$\mathbf{e}_n \times \delta \hat{\mathbf{A}}_b \big|_{S_b} = 0. \tag{20}$$

Ultimately, the growth rate of unstable modes in the presence of a resistive wall will be expressed explicitly in terms of δW_∞ and δW_b.

III. The Resistive Wall Case

In this section, we replace the perfectly conducting wall at S_b with a thin resistive wall characterized by a conductivity σ and thickness d (see Fig. 1). By exploiting the thin wall assumption, we then derive a relatively simple variational principle describing the stability of external modes in the presence of a resistive wall.

A. Time and Length Scale Orderings

The critical insight in the analysis of resistive wall MHD problems is that instabilities, if they exist, will be slowly growing modes with growth rates γ comparable to the resistive diffusion time of the wall τ_D:

$$\gamma \sim \frac{1}{\tau_D}. \tag{21}$$

Here, $\tau_D = \mu_0 \sigma \bar{b} d$ and $\bar{b}$ is a measure of the average radius of the vacuum chamber. Due to the scaling in Eq. (21)

$$\gamma \ll \gamma_{MHD} \tag{22}$$

where $\gamma_{MHD}^2 = -\delta W_\infty / K$ is the characteristic ideal MHD growth rate with the wall at infinity. For the Alcator C-Mod tokamak $\bar{b} \sim 0.4\,\mathrm{m}$, $d \sim 0.025\,\mathrm{m}$, and $1/\sigma \sim 69.5 \times 10^{-8}\,\Omega \cdot \mathrm{m}$ so $\gamma \sim 55\,\mathrm{Hz}$. Typically $\gamma_{MHD} \sim 2 \times 10^6\,\mathrm{Hz}$ so Eq. (22) is usually well satisfied.

The thin wall model assumes

$$d \ll \bar{b}. \tag{23}$$

However, it is necessary to ensure that d is not so small that Eq. (22) is violated.

The orderings given by Eqs. (21)–(23) imply that plasma inertial effects are negligible on the time scale of interest. This leads to a substantial simplification in the analysis. In particular, the equation describing the linearized plasma behavior is just

$$\mathbf{F}(\xi) = 0 \tag{24}$$

where $\mathbf{F}$ is the well-known force operator of ideal MHD.

B. Magnetic Field Solutions

As Fig. 1 shows, the volume surrounding the plasma is divided into three parts: an inner vacuum region, the resistive wall, and an outer vacuum region. The governing equations and boundary conditions for the fields in those three regions are given as follows.

1. Vacuum Region Analysis

The vector potentials for the inner and outer vacuum regions $\delta\hat{\mathbf{A}}_i$ and $\delta\hat{\mathbf{A}}_o$ satisfy

$$\nabla \times \nabla \times \delta\hat{\mathbf{A}}_i = 0, \tag{25}$$

$$\nabla \times \nabla \times \delta\hat{\mathbf{A}}_o = 0. \tag{26}$$

Furthermore, at the plasma surface, the boundary condition on $\delta\hat{\mathbf{A}}_i$ is given by

$$\mathbf{e}_n \times \delta\hat{\mathbf{A}}_i \,|_{S_p} = -(\mathbf{e}_n \cdot \xi)\mathbf{B} \tag{27}$$

while, far from the wall, the corresponding condition on $\delta\hat{\mathbf{A}}_o$ has the form

$$\delta\hat{\mathbf{A}}_o \,|_{\infty} = 0. \tag{28}$$

For a real wall, no surface currents exist on either the interior or exterior surfaces. Consequently the tangential components of both $\delta\mathbf{E}$ and $\delta\mathbf{B}$ must be continuous across both interfaces. In terms of $\delta\mathbf{A}$ these boundary conditions are given by

$$\begin{aligned} [\mathbf{e}_n \times \delta\mathbf{A}]_{S_i} &= 0 \qquad [\mathbf{e}_n \times \delta\mathbf{A}]_{S_o} = 0, \\ [\mathbf{e}_n \times \nabla \times \delta\mathbf{A}]_{S_i} &= 0 \quad [\mathbf{e}_n \times \nabla \times \delta\mathbf{A}]_{S_o} = 0. \end{aligned} \tag{29}$$

Here, S_i and S_o represent the interior and exterior faces of the conducting wall respectively.

2. Resistive Wall Analysis

The fields within the resistive wall are calculated as follows. First, the electric and magnetic fields are expressed as

$$\delta \mathbf{E}_w = -\frac{\partial \delta \mathbf{A}_w}{\partial t}, \tag{30}$$

$$\delta \mathbf{B}_w = \nabla \times \delta \mathbf{A}_w \tag{31}$$

indicating that $\phi = 0$ has been chosen as the gauge condition. The wall itself is considered to be a thin metallic shell of uniform thickness d and uniform conductivity σ. Hence, in the wall $\delta \mathbf{J}_w = \sigma \delta \mathbf{E}_w$. Using the assumption that all perturbed quantities vary as $\delta Q(\mathbf{r}, t) = \delta Q(\mathbf{r}) \exp(\gamma t)$, it follows from Ampere's law that $\delta \mathbf{A}_w$ satisfies

$$\nabla \times \nabla \times \delta \mathbf{A}_w = -\mu_0 \sigma \gamma \delta \mathbf{A}_w. \tag{32}$$

The solution for $\delta \mathbf{A}_w$ can be found analytically for an arbitrarily shaped wall by exploiting the thin wall assumption. Two steps are required, one which separates normal from tangential derivatives, and the other which results in the expansion of $\delta \mathbf{A}_w$ with respect to the perpendicular distance into the wall.

Consider the separation of normal and tangential derivatives. To do this in a convenient manner we will represent points within the wall using the parameterization

$$\mathbf{r} = \mathbf{r}_i + u d \mathbf{e}_n \tag{33}$$

where $\mathbf{r}_i$ is a vector representing the inner surface of the conducting wall and, in this context, $\mathbf{e}_n$ is the unit vector normal to the inner surface of the wall. The normalized length u represents perpendicular distance measured outward from the inner surface of the wall. Thus, $u = 0$ and $u = 1$ correspond to S_i and S_o respectively.

Using the coordinate transformation in Eq. (33) and invoking the thin wall assumption [Eq. (23)] allow the gradient operator to be written

$$\nabla = \frac{\mathbf{e}_n}{d}\frac{\partial}{\partial u} + \nabla_S \tag{34}$$

where ∇_S only involves derivatives tangent to the surface of the wall.

In the limit of a thin wall, it is assumed that $\delta\mathbf{A}_w$ varies much more rapidly normal to the wall than tangent to it. Therefore, we formally introduce a small parameter $\delta \sim d/\bar{b}$ and assume the following ordering for the derivatives

$$\frac{\partial}{\partial u} \sim 1, \tag{35}$$

$$\bar{b}\nabla_S \sim 1. \tag{36}$$

The above ordering can now be used to define an expansion for $\delta\mathbf{A}_w$ in a manner entirely analogous to the "constant-ψ" approximation of tearing mode theory.[11] The appropriate expansion is given by

$$\delta\mathbf{A}_w(u, S) = \delta\mathbf{A}_{w0}(S) + \delta\mathbf{A}_{w1}(u, S) + \cdots \tag{37}$$

where $\delta\mathbf{A}_{w1}/\delta\mathbf{A}_{w0} \sim \delta$ and $F(S)$ denotes a functional dependence only on tangential surface coordinates. The corresponding maximal ordering for γ requires

$$\mu_0\sigma\gamma\bar{b}d \sim 1 \tag{38}$$

which is seen to be compatible with Eq. (21).

After a short calculation, it can be shown that the leading order contribution to Eq. (32) reduces to

$$\frac{\partial^2}{\partial u^2}(\mathbf{e}_n \times \delta\mathbf{A}_{w1}) = \mu_0\sigma\gamma d^2(\mathbf{e}_n \times \delta\mathbf{A}_{w0}). \tag{39}$$

The solution of Eq. (39) is easily found to be

$$\mathbf{e}_n \times \delta\mathbf{A}_{w1} = \mathbf{a}_1(S) + \mathbf{c}_1(S)u + \mu_0\sigma\gamma d^2(\mathbf{e}_n \times \delta\mathbf{A}_{w0})(u^2/2) \tag{40}$$

where $\mathbf{a}_1$ and $\mathbf{c}_1$ are integration constants, each of order δ.

A set of jump conditions involving $\delta\hat{\mathbf{A}}_i$ and $\delta\hat{\mathbf{A}}_o$ can be found by applying the boundary conditions given by Eq. (29). The results can be written, correct to leading order, as follows

$$\mathbf{e}_n \times \delta\hat{\mathbf{A}}_i \mid_{S_i} = \mathbf{e}_n \times \delta\mathbf{A}_{w0}, \tag{41}$$

$$\mathbf{e}_n \times \delta\hat{\mathbf{A}}_o \mid_{S_o} = \mathbf{e}_n \times \delta\mathbf{A}_{w0}, \tag{42}$$

$$\mathbf{e}_n \times \nabla \times \delta\hat{\mathbf{A}}_i \mid_{S_i} = \frac{1}{d}\mathbf{e}_n \times \mathbf{c}_1, \tag{43}$$

$$\mathbf{e}_n \times \nabla \times \delta\hat{\mathbf{A}}_o \mid_{S_o} = \frac{1}{d}\mathbf{e}_n \times \mathbf{c}_1 + \mu_0\sigma\gamma d\mathbf{e}_n \times (\mathbf{e}_n \times \delta\mathbf{A}_{w0}). \tag{44}$$

By subtracting Eq. (41) from Eq. (42) and Eq. (43) from Eq. (44) we see that the effect of the resistive wall explicitly appears only as a contribution to the jump conditions on $\delta\hat{\mathbf{A}}_i$ and $\delta\hat{\mathbf{A}}_o$ across the wall. Specifically, we obtain

$$\mathbf{e}_n \times \delta\hat{\mathbf{A}}_i \mid_{S_b} = \mathbf{e}_n \times \delta\hat{\mathbf{A}}_o \mid_{S_b}, \tag{45}$$

$$\mathbf{e}_n \times (\mathbf{e}_n \times \nabla \times \delta\hat{\mathbf{A}}_i) \mid_{S_b} = \mathbf{e}_n \times (\mathbf{e}_n \times \nabla \times \delta\hat{\mathbf{A}}_o) \mid_{S_b} + \mu_0\sigma\gamma d(\mathbf{e}_n \times \delta\hat{\mathbf{A}}) \mid_{S_b}. \tag{46}$$

C. Resistive Wall Variational Principle

In analogy to the derivation of the Energy Principle, Eq. (24) can be used to define a Lagrangian representing the dynamics of a plasma in the presence of a resistive wall:

$$\mathcal{L} \equiv \int_{V_p} \xi \cdot \mathbf{F}(\xi)\, dV = 0. \tag{47}$$

This Lagrangian can be rewritten in the more familiar form

$$\mathcal{L} = \delta W_F + \frac{1}{2}\int_{S_p} (\mathbf{e}_n \cdot \xi)\left(\frac{\hat{\mathbf{B}} \cdot \delta\hat{\mathbf{B}}}{\mu_0}\right) dS. \tag{48}$$

For the purposes of this analysis, it is convenient to write $\mathcal{L}$ in still another way. This is accomplished by noting the following identities

$$\begin{aligned}
\delta W_V^{(i)} &= \frac{1}{2\mu_0}\int_{V_i} |\nabla \times \delta\hat{\mathbf{A}}_i|^2\, dV \\
&= \frac{1}{2}\int_{S_p} (\mathbf{e}_n \cdot \xi)\left(\frac{\hat{\mathbf{B}}\cdot\delta\hat{\mathbf{B}}}{\mu_0}\right) dS - \\
&\quad \frac{1}{2\mu_0}\int_{S_b} (\mathbf{e}_n \times \delta\hat{\mathbf{A}}_i)\cdot \mathbf{e}_n \times (\mathbf{e}_n \times \nabla \times \delta\hat{\mathbf{A}}_i)\, dS, \qquad (49)
\end{aligned}$$

$$\begin{aligned}
\delta W_V^{(o)} &= \frac{1}{2\mu_0}\int_{V_o} |\nabla \times \delta\hat{\mathbf{A}}_i|^2\, dV \\
&= \frac{1}{2\mu_0}\int_{S_b} (\mathbf{e}_n \times \delta\hat{\mathbf{A}}_o)\cdot \mathbf{e}_n \times (\mathbf{e}_n \times \nabla \times \delta\hat{\mathbf{A}}_o)\, dS \qquad (50)
\end{aligned}$$

where V_i and V_o refer to the vacuum regions inside and outside the resistive wall respectively (see Fig. 1). In addition, the relevant governing equations and boundary conditions [Eqs. (25)–(28)] for $\delta\hat{\mathbf{A}}_i$ and $\delta\hat{\mathbf{A}}_o$ have been applied in the derivation of Eqs. (49) and (50).

Using the resistive wall jump conditions in Eqs. (45) and (46), the desired form of $\mathcal{L}$ can be obtained:

$$\mathcal{L} = \delta W_F + \delta W_V^{(i)} + \delta W_V^{(o)} + \frac{\sigma\gamma d}{2}\int_{S_b} |\mathbf{e}_n \times \delta\hat{\mathbf{A}}|^2\, dS. \qquad (51)$$

Note that in the limit of marginal stability ($\gamma \to 0$), Eq. (51) reduces to the ideal MHD potential energy with a wall at infinity δW_∞. Thus, in this limit, the true eigenfunction of the resistive system approaches the vacuum solution for the ideal system $\delta\hat{\mathbf{A}}_\infty$. The conclusion is that the marginal stability threshold of the resistive system $\delta W_\infty = 0$ is indeed the exact threshold.

To verify the validity of the variational principle, we evaluate $\delta\mathcal{L}$ and set it to zero. A relatively lengthy calculation yields

$$\begin{aligned}
\delta\mathcal{L} \;=\; & \int_{V_p} \delta\xi \cdot \mathbf{F}(\xi)\, dV + \\
& \frac{1}{\mu_0}\int_{V_i} \delta(\delta\hat{\mathbf{A}}_i)\cdot \nabla\times\nabla\times\delta\hat{\mathbf{A}}_i\, dV + \\
& \frac{1}{\mu_0}\int_{V_o} \delta(\delta\hat{\mathbf{A}}_o)\cdot \nabla\times\nabla\times\delta\hat{\mathbf{A}}_o\, dV + \\
& \int_{S_p} (\mathbf{e}_n\cdot\delta\xi)\left(\frac{(\hat{\mathbf{B}}\cdot\delta\hat{\mathbf{B}}-\mathbf{B}\cdot\delta\mathbf{B})}{\mu_0}\right) dS + \\
& \frac{1}{\mu_0}\int_{S_b} (\mathbf{e}_n\times\delta(\delta\hat{\mathbf{A}}))\cdot\Big[\mathbf{e}_n\times(\mathbf{e}_n\times\nabla\times\delta\hat{\mathbf{A}}_o)+ \\
& \mu_0\sigma\gamma d(\mathbf{e}_n\times\delta\hat{\mathbf{A}})-\mathbf{e}_n\times(\mathbf{e}_n\times\nabla\times\delta\hat{\mathbf{A}}_i)\Big]\, dS. \qquad (52)
\end{aligned}$$

From Eq. (52), it can be seen that for the volume contributions to vanish, Eqs. (24), (25), and (26) must be satisfied. In addition, the surface contributions give rise to the two natural boundary conditions

$$\hat{\mathbf{B}}\cdot\delta\hat{\mathbf{B}}\,\big|_{S_p} \;=\; \mathbf{B}\cdot\delta\mathbf{B}\,\big|_{S_p}, \qquad (53)$$

$$\begin{aligned}
\mathbf{e}_n\times(\mathbf{e}_n\times\nabla\times\delta\hat{\mathbf{A}}_i)\,\big|_{S_b} \;=\; & \mathbf{e}_n\times(\mathbf{e}_n\times\nabla\times\delta\hat{\mathbf{A}}_o)\,\big|_{S_b} + \\
& \mu_0\sigma\gamma d(\mathbf{e}_n\delta\hat{\mathbf{A}}\,\big|_{S_b}. \qquad (54)
\end{aligned}$$

Finally, Eq. (52) was derived assuming the boundary conditions

$$\mathbf{e}_n\times\delta\hat{\mathbf{A}}_i\,\big|_{S_p} = -(\mathbf{e}_n\cdot\xi)\mathbf{B}\,\big|_{S_p}, \qquad (55)$$

$$\mathbf{e}_n\times\delta\hat{\mathbf{A}}_i\,\big|_{S_b} = \mathbf{e}_n\times\delta\hat{\mathbf{A}}_o\,\big|_{S_b}, \qquad (56)$$

$$\delta\hat{\mathbf{A}}_o\,\big|_{\infty} = 0 \qquad (57)$$

are exactly satisfied. Since the set of relations that causes $\mathcal{L}$ to be stationary corresponds to the previously described governing equations and boundary conditions, we conclude that Eq. (51) represents the desired variational principle.

IV. Resistive Wall Growth Rates

In situations where $\delta W_\infty < 0$ and $\delta W_b > 0$ we can obtain an accurate estimate of the growth rate by the use of trial functions. A convenient choice for $\delta\hat{\mathbf{A}}_i$ and $\delta\hat{\mathbf{A}}_o$ that takes into account the nature of the boundary conditions can be written as

$$\delta\hat{\mathbf{A}}_i = c_1\delta\hat{\mathbf{A}}_\infty + c_2\delta\hat{\mathbf{A}}_b, \tag{58}$$

$$\delta\hat{\mathbf{A}}_o = c_3\delta\hat{\mathbf{A}}_\infty. \tag{59}$$

The coefficients c_1, c_2 and c_3 are initially arbitrary. However, two constraints are imposed on $\delta\hat{\mathbf{A}}_i$ and $\delta\hat{\mathbf{A}}_o$ by the conditions described by Eqs. (55)–(57). First, since $\delta\hat{\mathbf{A}}_\infty$ and $\delta\hat{\mathbf{A}}_b$ satisfy the same boundary condition on S_p as given by Eqs. (7) and (15), Eq. (55) implies that

$$c_1 + c_2 = 1. \tag{60}$$

Next, since $\mathbf{e}_n \times \delta\hat{\mathbf{A}}_b \big|_{S_b} = 0$ from Eq. (14), it follows that Eq. (56) requires

$$c_1 = c_3. \tag{61}$$

The last condition, corresponding to Eq. (57), is automatically satisfied since $\delta\hat{\mathbf{A}}_\infty \big|_\infty = 0$ as required by Eq. (6). Thus, of the three coefficients—c_1, c_2, and c_3—only one is independent.

Using the properties of the vacuum solutions, one can easily evaluate $\mathcal{L}$ as given by Eq. (51). A short calculation yields

$$\begin{aligned}
\mathcal{L} \;=\; & \delta W_F + c_1(c_1+c_2)\delta W_V^{(\infty)} + c_2(c_1+c_2)\delta W_V^{(b)} - \\
& \frac{(c_1^2 - c_3^2)}{2\mu_0}\int_{S_b} (\mathbf{e}_n \times \delta\hat{\mathbf{A}}_\infty)\cdot \mathbf{e}_n \times (\mathbf{e}_n \times \nabla \times \delta\hat{\mathbf{A}}_\infty)\, dS - \\
& \frac{c_1 c_2}{2\mu_0}\int_{S_b} (\mathbf{e}_n \times \delta\hat{\mathbf{A}}_\infty)\cdot \mathbf{e}_n \times (\mathbf{e}_n \times \nabla \times \delta\hat{\mathbf{A}}_b)\, dS + \\
& \frac{c_1\gamma\sigma d}{2}\int_{S_b} |\mathbf{e}_n \times \delta\hat{\mathbf{A}}_\infty|^2\, dS.
\end{aligned} \tag{62}$$

This expression can be simplified by eliminating c_1 and c_3 in terms of c_2 by means of Eqs. (60) and (61) and by making use of the identity

$$\nabla \cdot (\delta\hat{\mathbf{A}}_\infty \times \nabla \times \delta\hat{\mathbf{A}}_b + \delta\hat{\mathbf{A}}_b \times \nabla \times \delta\hat{\mathbf{A}}_\infty) = 0. \tag{63}$$

This procedure leads to

$$\mathcal{L} = \delta W_\infty + c_2^2(\delta W_b - \delta W_\infty) + \frac{\sigma\gamma d(1-c_2)}{2}\int_{S_b} |\mathbf{e}_n \times \delta\hat{\mathbf{A}}_\infty|^2\, dS. \tag{64}$$

Observe that $\mathcal{L}$ is a simple quadratic equation in terms of the variational parameter c_2. It is now straightforward to determine c_2 by setting $\partial\mathcal{L}/\partial c_2 = 0$. The resulting value of c_2 is substituted back into $\mathcal{L}$ which is then set to zero. The equation $\mathcal{L} = 0$ can be solved for the growth rate γ yielding

$$\gamma\tau_D = -\frac{\delta W_\infty}{\delta W_b} \tag{65}$$

where

$$\tau_D = \mu_0\sigma d\bar{b} \tag{66}$$

and $\bar{b}$ is explicitly written

$$\bar{b} = \frac{\frac{1}{2\mu_0}\int_{S_b} |\mathbf{e}_n \times \delta\hat{\mathbf{A}}_\infty|^2\, dS}{(\delta W_b - \delta W_\infty)} \tag{67}$$

$$= \frac{\int_{S_b} |\mathbf{e}_n \times \delta\hat{\mathbf{A}}_\infty|^2\, dS}{\int_{S_b}(\mathbf{e}_n \times \delta\hat{\mathbf{A}}_\infty)\cdot \mathbf{e}_n \times (\mathbf{e}_n \times \nabla \times \delta\hat{\mathbf{A}}_b)\, dS}. \tag{68}$$

Equations (65)–(68) represent a generalization of the result derived by Freidberg for the circular RFP.[12]

Due to the variational nature of the equations, the substitution of a trial function into Eq. (65) and the variation of that trial function so as to maximize γ (or equivalently, minimize $\mathcal{L}$) provides an accurate estimate of the resistive wall growth rate in terms of quantities relating to the ideal system with and without a perfectly conducting wall. An important conclusion from Eq. (65) is

that a system which is unstable with a wall at infinity $\delta W_\infty < 0$ but stable with a perfectly conducting wall near the plasma $\delta W_b > 0$ will always be unstable to a slowly growing real mode if the wall is resistive. The characteristic growth time is comparable to the resistive diffusion time through the wall. Note as well that, as one would expect, $\gamma \to 0$ as $\delta W_\infty \to 0$. In other words, the resistive growth rate vanishes when the plasma is ideally stable with a wall at infinity.

V. Non-Ideal Effects on Resistive Wall Instabilities

The analysis just presented shows that a resistive wall leads to slowly growing modes with zero real frequency. It can be argued that the addition of non-ideal effects into the plasma model may cause the natural modes of the system to develop a real part in the frequency. In this situation, the resistive wall must respond to an AC signal. If the frequency is high enough so that the skin depth is smaller than the wall thickness, the resistive wall would behave as a perfect conductor; wall stabilization would persist even in the presence of a resistive wall. Finite Larmor radius (FLR) and plasma rotation are two such effects which produce a real frequency for unstable ideal MHD modes.

This appealing argument does not apply to resistive wall instabilities. To show this consider the analysis of Pearlstein and Freidberg[13] who derived the following variational principle for MHD stability including FLR and plasma rotation in arbitrary near θ pinch geometry:

$$\mathcal{L} = \delta W - \frac{1}{2}\int_{V_p} \rho\xi_\perp \cdot \mathbf{D} \cdot \xi_\perp \, dV. \tag{69}$$

Here, $\xi_\perp$ must satisfy $\nabla \cdot \xi_\perp = 0$ and $\mathbf{D}$ is given by

$$\mathbf{D} = \begin{pmatrix} T & i(T-\omega^2)/m \\ -i(T-\omega^2)/m & T \end{pmatrix} \tag{70}$$

where m is the dominant poloidal harmonic mode number and

$$T = (\omega - m\Omega)\left[\omega - m(\Omega + \Omega_{*i}) - \frac{\beta}{2} m\Omega_{*i}\right]. \tag{71}$$

In Eq. (71), $\Omega_{*i} = -(1/enrB)(dp_i/dr)$ is the ion diamagnetic drift velocity representing FLR effects and Ω represents the rotation velocity of the plasma. For ideal MHD $\Omega = \Omega_{*i} = 0$ and $T = \omega^2$.

The critical point to recognize is that the new effects enter the calculation as modifications to the inertia term. Thus, if one again considers slowly growing modes, $|\omega| \sim 1/\tau_D \ll \gamma_{MHD}$ then FLR and rotational effects are unimportant if

$$\Omega_{*i}/\tau_D \ll \gamma^2_{MHD}, \tag{72}$$

$$\Omega/\tau_D \ll \gamma^2_{MHD}. \tag{73}$$

Specifically, when Eqs. (72) and (73) are satisfied, as they are in most practical applications, FLR and rotational effects modify T from its ideal value

$$T = \omega^2 \sim 1/\tau_D^2 \approx 0 \tag{74}$$

to

$$T \approx m^2\Omega[\Omega + (1 + \beta/2)\Omega_{*i}]; \tag{75}$$

that is, FLR and rotation produce small corrections to the potential energy δW but do not modify the frequency dependence of the eigenvalue problem.

The situation is summarized in Fig. 2 where we have illustrated typical spectral plots for the systems under discussion. Figure 2a shows the situation with the wall at infinity and predicts ideal instability ($\mathrm{Re}\,\gamma > 0$). In Fig. 2b a perfectly conducting wall is brought close enough to the plasma to provide wall stabilization ($\mathrm{Re}\,\gamma = 0$). Figure 2c shows the effect of substituting a resistive wall in place of the perfectly conducting wall. The ideal wall stabilized modes become slightly damped ($\mathrm{Re}\,\gamma < 0$). This is the "AC wall stabilization" previously discussed. However, a new, purely growing unstable mode develops out of the origin ($\mathrm{Re}\,\gamma > 0$) corresponding to the resistive wall instability.

The conclusion is that FLR effects and plasma rotation do not produce any significant modification to resistive wall instabilities. A similar conclusion applies to electron diamagnetic effects characterized by the parameter $\omega_{*e} = m\Omega_{*e}$, although for a different reason; that is, since unstable ideal MHD modes satisfy $E_\parallel = 0$, parallel electron dynamics do not play an important role. Hence, ω_{*e} does not affect ideal MHD instabilities. However, for resistive tearing modes, which depend sensitively on $E_\parallel = \eta J_\parallel \neq 0$, parallel electron dynamics play an important role, causing a real part to the frequency of order $\mathrm{Re}\omega \sim \omega_{*e}$. For these modes, AC wall stabilization should be an important stabilizing influence.

VI. Axisymmetric Stability of the Straight Ellipse

As an application of the preceeding analysis, we will now consider the axisymmetric ($n = 0$) stability of a straight elliptical tokamak possessing a peaked current density profile but negligible plasma pressure. First, ideal stability boundaries will derived by assuming the presence of a perfectly conducting wall surrounding the plasma. Then, these results will be used in Eqs. (65)–(68) to calculate the growth rate of modes driven unstable by the presence of a resistive wall.

The study of the effect of resistive vacuum vessels on axisymmetric modes is a particularly important problem since several current or proposed experimental devices are characterized by relatively large plasma elongations and discharge times. The size of the growth rate resulting from a given vessel configuration gives an estimate of the requirements for an active feedback system or additional passive stabilizers needed to keep the plasma position within acceptable bounds.

The ideal axisymmetric stability of the straight elliptical tokamak with a flat current density profile has been studied by several authors.[1–3] The additional effects of a specific peaked current density profile and finite beta were modeled by Laval and Pellat[14] and Haas[3] respectively. Wesson[8] included the effect of a resistive wall while retaining the assumption of a flat current density profile.

Here, we first recover the flat current profile results and then extend them to include the effects of arbitrary current density profiles.

A. Equilibrium

We consider a straight elliptical tokamak with minor radius a, vertical elongation at the plasma surface κ_a, and length $2\pi R_0$. Due to the assumption of this simple plasma geometry along with that of zero plasma pressure, the internal plasma flux surface shapes S_ψ can be accurately parameterized by a series of nested ellipses with elongations varying quadratically between κ_0 at the magnetic axis and κ_a at the plasma surface. This topological model has been found to agree quite well with exact solutions to the Grad-Shafranov equation obtained using the NEQ MHD equilibrium code.[15] In addition, the model is simple enough to preserve the desired analytic nature of the calculation.

In the nested elliptical flux surface model, S_ψ is parameterized by

$$S_\psi = \{R(\rho, \mu), Z(\rho, \mu)\} \tag{76}$$

where (R, φ, Z) form a right-handed cylindrical coordinate system and

$$R(\rho, \mu) = R_0 + a\rho\cos\mu, \tag{77}$$

$$Z(\rho, \mu) = a\rho\kappa(\rho)\sin\mu, \tag{78}$$

$$\kappa(\rho) = \kappa_0 + (\kappa_a - \kappa_0)\rho^2, \tag{79}$$

$$\psi = \psi(\rho). \tag{80}$$

The parameter ρ is a flux surface label while the parameter μ is an angular variable. Without loss of generality, it can be assumed that ρ varies between 0 (representing the magnetic axis) and 1 (representing the plasma surface) while μ varies between 0 and 2π (this variation representing a complete poloidal circuit around a flux surface). Since ρ labels flux surfaces, the flux function ψ is

explicitly considered to be only a function of that variable [see Eq. (80)]. The straight limit is formally applied by letting $a/R_0 \to 0$.

The central elongation κ_0 depends on the details of the current density profile and must, in general, be obtained through a numerical calculation. As an example of typical results, consider Fig. 3 which was constructed using the variational equilibrium code ePFC[16] for a series of plasmas characterized by $a = 0.5\,\mathrm{m}$, $R_0 = 10.0\,\mathrm{m}$, $I_p = 1.0\,\mathrm{MA}$, and $\kappa_a = 1.5$ and 2.0. Figure 3a shows the variation of a parameter λ related to the central elongation

$$\lambda \equiv \frac{\kappa_a - \kappa_0}{\kappa_a} \tag{81}$$

with another parameter α related to the width of the axial current density profile (see Fig. 3b.) Specifically, the variation in the axial current density J_φ with ψ is given by

$$J_\varphi / J_{\varphi 0} = \frac{\exp[-\alpha(1-\tilde{\psi})] - \exp(-\alpha)}{1 - \exp(-\alpha)} \tag{82}$$

where $\tilde{\psi} = \psi/\psi_0$, ψ_0 is the flux at the magnetic axis, and $J_{\varphi 0}$ is the axial current density at the magnetic axis. Notice that when the current density profile is flat, $\kappa_0 = \kappa_a$ ($\lambda = 0$). Otherwise, the steeper the profile, the smaller κ_0 becomes in relation to κ_a ($\lambda > 0$). Finally, notice that λ increases more rapidly with α as κ_a increases.

B. Calculation of Energy Integrals

1. Calculation of Fluid Energy

It has been rigorously demonstrated[1,2] that the rigid vertical shift

$$\xi = \xi_Z \, \mathbf{e}_Z \tag{83}$$

is the most unstable axisymmetric trial function for the straight elliptical tokamak. Therefore, we will evaluate the energy integrals under this assumption. Note, however, that the rigid vertical shift is a considerably less accurate trial function for more realistic shapes like finite aspect ratio dees.[4,16] For these geometries, a trial function like that described in Refs. 4 and 16 is required in order to obtain reliable results.

Under the assumption of a rigid vertical shift, δW_F [Eq. (2)] takes on the particularly compact form

$$\delta W_F = \frac{\xi_Z^2}{2\mu_0} \int_{S_p} (\mathbf{e}_n \cdot \mathbf{e}_Z)(\mathbf{B} \cdot \nabla(\mathbf{e}_Z \cdot \mathbf{B}))\, dS. \tag{84}$$

This expression can, in turn, be simply evaluated using the equilibrium information in Eqs. (77)–(80) to give

$$\delta W_F = -\frac{\pi^2 \xi_Z^2}{\mu_0 a^2 R_0 \kappa_a} \left[\frac{d\psi}{d\rho}(1)\right]^2 \left[\frac{1+\lambda}{(1+2\lambda)^{3/2}}\right]. \tag{85}$$

2. Calculation of Vacuum Energy: Perfectly Conducting Wall

Due to the rigid vertical shift assumption, the vacuum energy [Eq. (12)] takes on a simple form as well

$$\delta W_V^{(b)} = \frac{\xi_Z}{2\mu_0} \int_{S_p} (\mathbf{e}_n \cdot \mathbf{e}_Z)(\mathbf{e}_t \cdot \delta\hat{\mathbf{B}})(\mathbf{e}_t \cdot \mathbf{B})\, dS \tag{86}$$

where $\mathbf{e}_t$ is a unit vector tangent to the plasma surface.

To evaluate $\delta W_V^{(b)}$ it is necessary to solve for $\delta\hat{\mathbf{B}}$ in the vacuum region between the plasma and the wall (here assumed to be perfectly conducting). Even in the straight limit, this is generally a difficult task due to the complexity of Eq. (13). However, if attention is focused on a special class of wall shapes, Eq. (13) can be transformed into a very simple form and solved analytically.

This transformation is accomplished by introducing the following vacuum coordinate system[3]:

$$R(u, \mu) = R_0 + a'(\sinh u \cos \mu), \tag{87}$$

$$Z(u, \mu) = a'(\cosh u \sin \mu) \tag{88}$$

where $u = u_a$ is assumed to parameterize the plasma surface and

$$u_a = \coth^{-1} \kappa_a, \tag{89}$$

$$a' = a/\sinh u_a. \tag{90}$$

For the sake of convenience, it will be assumed that the wall surface also lies on a constant-u surface: specifically, $u = u_b$ where $u_b > u_a$. Examples of the wall shapes produced by this parameterization are shown in Fig. 4. In the figure, the plasma-wall separation is labeled using the quantity (originally suggested by Haas[3])

$$t \equiv e^{2(u_a - u_b)}. \tag{91}$$

Note that t is related to the ratio of the cross-sectional area of the plasma to the area enclosed by the wall. Hence, $t = 1$ corresponds to the wall lying on the plasma surface while $t \to 0$ corresponds to the wall being moved to infinity.

In the above coordinate system (and in the straight limit) Eq. (13) simplifies to

$$\frac{\partial^2 \delta \hat{A}_{b\varphi}}{\partial u^2} + \frac{\partial^2 \delta \hat{A}_{b\varphi}}{\partial \mu^2} = 0. \tag{92}$$

Equation (92) is simply Laplace's equation in "rectangular" coordinates. Hence, $\delta \hat{A}_{b\varphi}$ can be found analytically in terms of a Fourier series that, with little error, can be truncated to one term due to fast convergence.

Once the vacuum field is known, we find from Eq. (86) that

$$\delta W_V^{(b)} = \frac{4\pi^2 \xi_Z^2}{\mu_0 a^2 R_0 \kappa_a^2 (1 + 2\lambda + \sqrt{1 + 2\lambda})^2} \left[\frac{d\psi}{d\rho}(1)\right]^2 \left[\frac{1+t}{1-t}\right]. \tag{93}$$

3. Calculation of Vacuum Energy: No Wall

By a very similar set of calculations, it is straightforward to analyze the case where no wall is present. We find

$$\delta W_V^{(\infty)} = \frac{4\pi^2 \xi_Z^2}{\mu_0 a^2 R_0 \kappa_a^2 (1+2\lambda+\sqrt{1+2\lambda})^2} \left[\frac{d\psi}{d\rho}(1)\right]^2, \tag{94}$$

$$\delta \hat{A}_{\infty\varphi}\,|_{u_b} = \frac{2\xi_Z t^{1/2} \sin\mu}{a R_0 \kappa_a (1+2\lambda+\sqrt{1+2\lambda})} \left[\frac{d\psi}{d\rho}(1)\right]. \tag{95}$$

C. Critical Position for a Perfectly Conducting Wall

We will now derive a condition giving the maximum distance a perfectly conducting wall can be placed while still ensuring at least marginal stability. This is found by setting $\delta W_b = 0$ and solving for t. The result is

$$t > \frac{\kappa_a G(\lambda) - 1}{\kappa_a G(\lambda) + 1} \tag{96}$$

where $G(\lambda)$ is a monotonically increasing function of λ defined by

$$G(\lambda) = \frac{1+\lambda}{4(1+2\lambda)^{3/2}} \left(1+2\lambda+\sqrt{1+2\lambda}\right)^2. \tag{97}$$

Note that the critical wall position in Eq. (96) does not depend explicitly on the shape of the flux function. Instead, the axisymmetric stability of the straight ellipse is only a function of the topology of the flux surfaces as specified by κ_a and λ.

Equations (96)–(97) extend the results of Laval and Pellat[14] to arbitrary current density profile. In the limit $\lambda \to 0$ the flat profile result obtained by Haas[3] is recovered. For non-zero values of λ, corresponding to peaked current density profiles, $G(\lambda)$ represents an effective enhancement of the plasma elongation. This, in turn, is known to represent a destabilizing factor for axisymmetric

modes in the straight ellipse.[3] Hence, the peaking of the current profile represents a destabilizing effect as well. This result is reasonable on physical grounds since the peaking of the current profile effectively moves the plasma current farther away from the stabilizing effects of the wall.

Figure 5 shows the variation in the critical wall position with κ_a and λ for the plasmas used to construct Fig. 3. Note that the variation with κ_a is relatively strong but that the variation with λ is relatively weak.

D. Growth Rate Estimate with a Resistive Wall

If a configuration with a perfectly conducting wall satisfies the stability condition given in Eq. (96), the substitution of a resistive wall results in a mode growing at a rate given by Eq. (65). Using Eq. (85) and Eqs. (93)–(95) in Eqs. (65)–(67) leads to a simple analytic expression for the growth rate

$$\gamma\tau_D = -\frac{2}{\mu_0\sigma\hat{b}d}\frac{\kappa_a G(\lambda) - 1}{(1-t)\kappa_a G(\lambda) - (1+t)} \tag{98}$$

where

$$\hat{b} = \frac{b}{\pi}\int_0^{2\pi} \sin^2\mu\sqrt{\kappa_b^2\cos^2\mu + \sin^2\mu}\,d\mu, \tag{99}$$

$b = a\sinh u_b/\sinh u_a$ is the minor radius of the wall, and $\kappa_b = \coth u_b$ is the elongation of the wall.

Note from Eq. (98) that as t approaches its critical position [obtained from Eq. (96)] γ approaches infinity. This is a consequence of the neglect of plasma inertial effects in Eq. (24). Neglecting plasma inertia is formally accomplished by letting the plasma mass density ρ approach zero. In this limit, the Alfvén velocity $v_A \propto 1/\rho^{1/2} \to \infty$ hence $\gamma_{MHD} \to \infty$.

Consider again the plasmas used to construct Fig. 3. Assuming a 0.025 m thick stainless-steel wall located at $t = 0.45$, it is possible to use Eq. (98) to construct a plot of γ as a function of λ for various plasma elongations. This

is shown in Fig. 6. Note that while the peaking of the current profile has a relatively small effect on the critical perfectly conducting wall position, it can substantially increase the resistive wall growth rates of axisymmetric modes, especially at larger elongations.

VII. Summary and Conclusions

In this paper we have considered the problem of external MHD mode stability in the presence of a resistive wall. Attention has been focused on the situation where the plasma is unstable with a wall at infinity ($\delta W_\infty < 0$), but stable with a sufficiently close-fitting perfectly conducting wall ($\delta W_b > 0$). When the perfectly conducting wall is replaced with one of finite conductivity, it was found that modes that were previously stable would start to grow at a rate related to the resistive diffusion time characterizing the wall. Since the growth rate of the resistive wall instability is much slower than ideal MHD growth rates, it was possible to neglect inertial effects in the equation of motion for the plasma. This simplified the analysis and also allowed the additional neglect of such non-ideal phenomena as FLR effects and plasma rotation.

On the basis of the above physics, a simple variational principle [Eq. (65)] giving the resistive wall growth rate in terms of quantities relating to the ideal system with and without a perfectly conducting wall was derived.

This variational principle was then used to investigate the axisymmetric ($n = 0$) stability of straight, zero pressure elliptical tokamaks with arbitrary current density profiles. For the cases examined, it was found that peaking of the current density profile had a small effect on the critical perfectly conducting wall position for the system but that it could dramatically enhance the resistive wall growth rate for the system.

The case of the straight elliptical tokamak demonstrated the utility of the variational principle derived here for easily gaining qualitative insight concerning resistive wall instabilities. More importantly, since the growth rate expression

depends on quantities relating to *ideal* MHD, it is possible that existing numerical ideal stability codes could be quickly and simply modified to give accurate resistive wall growth rate information.

As a final point, the simple variational principle derived here could be used as a theoretical starting point for more elaborate resistive wall problems. This has already proven to be the case in the development of a computer code to model axisymmetric stability in tokamaks in the presence of an arbitrary configuration of resistive conductors and feedback.[16]

Acknowledgements

The authors would like to acknowledge several very useful discussions with J. Wesson, T. Jensen, and J. P. Goedbloed concerning resistive wall instabilities. This research was performed in part in conjunction with the Magnetic Fusion Energy Technology Fellowship Program and the Fusion Energy Postdoctoral Research Program both of which are managed for the United States Department of Energy by Oak Ridge Associated Universities.

References

[1]G. Laval, R. Pellat, and J.S. Soule, Phys. Fluids **17** (1974) 835.

[2]R.L. Dewer, R.C. Grimm., J.L. Johnson, E.A. Frieman, G.M. Greene, and P.H. Rutherford, Phys. Fluids **17** (1974) 930.

[3]F.A. Haas, Nucl. Fusion **15** (1975) 407.

[4]L.C. Bernard, D. Berger, R. Gruber, and F. Troyon, Nucl. Fusion **18** (1978) 1331.

[5]J.A. Wesson, Nucl. Fusion **18** (1978) 87.

[6]D. Pfirsch and H. Tasso, Nucl. Fusion **11** (1971) 259.

[7]J.P. Goedbloed, D. Pfirsch, and H. Tasso, Nucl. Fusion **12** (1972) 649.

[8]J.A. Wesson, in Controlled Fusion and Plasma Physics (Proc. 7th Europ. Conf. Lausanne, 1975), Vol. 2, European Physical Society (1975) 102.

[9]S.C. Jardin, Phys. Fluids **21** (1978) 10.

[10]I.B. Bernstein, E.A. Frieman, M.D. Kruskal, and R.M. Kulsrud, Proc. R. Soc. London, Ser. A **244** (1958) 17.

[11]H.P. Furth, J. Kileen, and M.N. Rosaenbluth, Phys. Fluids **6** (1963) 459.

[12]J.P. Freidberg, *Ideal Magnetohydrodynamics*, Plenum Press (1987) 307.

[13]L.D. Pearlstein and J.P. Freidberg, Phys. Fluids **21** (1978) 1207.

[14]G. Laval and R. Pellat, in Controlled Fusion and Plasma Physics (Proc. 6th Europ. Conf. Moscow, 1973), Vol. 2, European Physical Society (1973) 640.

[15]D.J. Strickler, F.B. Miller, K.E. Rothe, and Y.-K.M. Peng, *Equilibrium Modeling of the TFCX Poloidal Field Coil System*, Oak Ridge National Lab. Report ORNL/FEDC-83/10 (1984).

[16]S.W. Haney, *Methods for the Design and Optimization of Shaped Tokamaks*, MIT Plasma Fusion Center Report PFC/RR-88-12 (Ph.D Thesis, 1988).

Figure Captions

Fig. 1: Plasma-resistive wall geometry.

Fig. 2: Spectral behavior of resistive wall instabilities: (a) wall at infinity, (b) perfectly conducting wall brought from infinity to a position near the plasma, (c) perfectly conducting wall replaced by resistive wall at the same location.

Fig. 3: Equilibrium information for model plasma configurations: (a) variation of central elongation parameter λ with current profile width parameter α for two values of plasma elongation κ_a, (b) variation of axial current density $J_\varphi/J_{\varphi 0}$ with normalized flux $\tilde{\psi}$ for several values of α.

Fig. 4: Variation in wall geometry as a function of Haas position parameter t. The solid line ($t = 1$) represents plasma surface. The dashed lines ($t < 1$) illustrate possible wall locations.

Fig. 5: Variation of the critical Hass wall position parameter t yielding marginal stability (in the presence of a perfectly conducting wall) with central elongation parameter λ for two values of plasma elongation κ_a.

Fig. 6: Variation of the resistive wall growth rate γ with central elongation parameter λ for two values of plasma elongation κ_a.

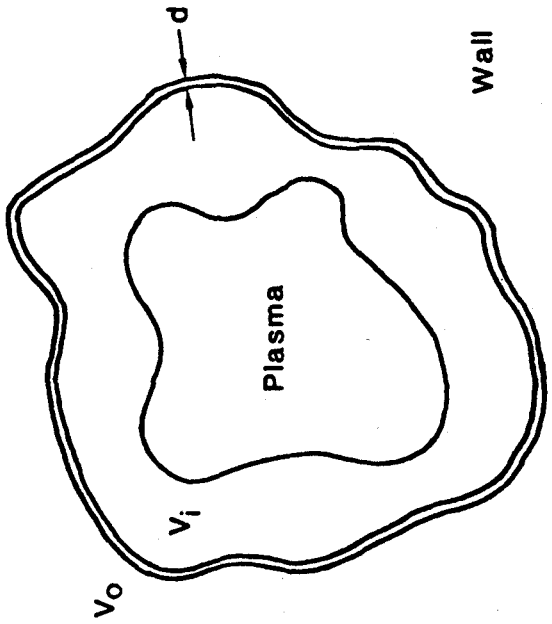

Haney and Freidberg, Fig. 1.

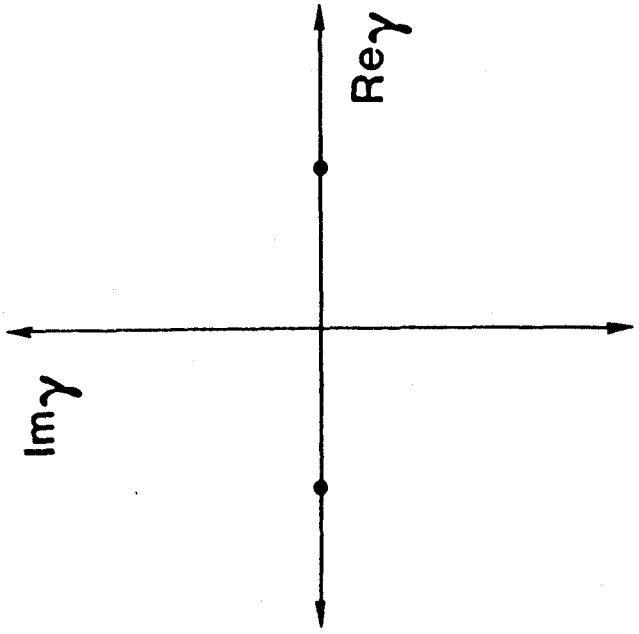

Haney and Freidberg, Fig. 2a.

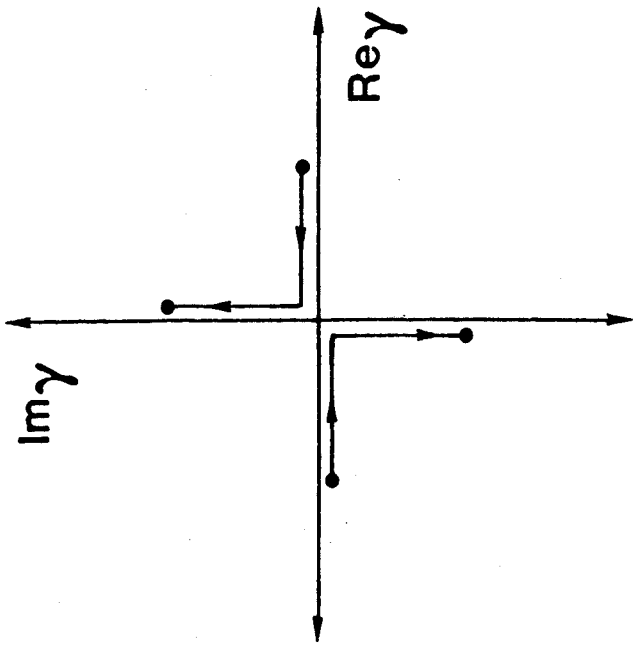

Haney and Freidberg, Fig. 2b.

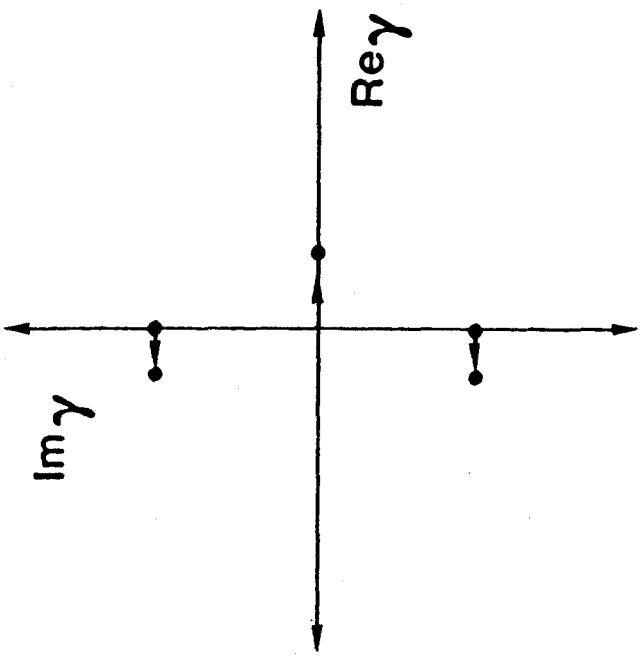

Haney and Freidberg, Fig. 2c.

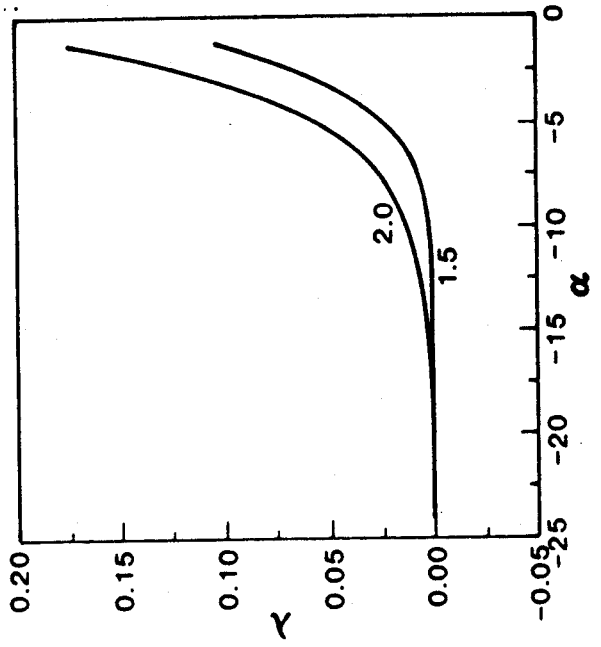

Haney and Freidberg, Fig. 3a.

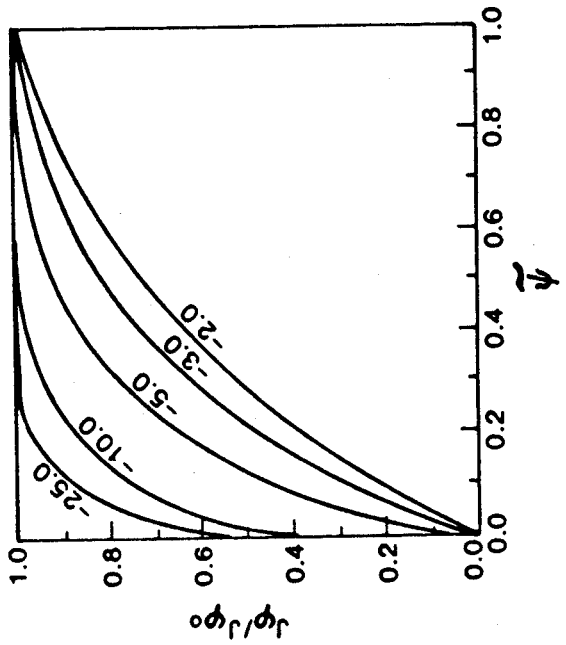

Haney and Freidberg, Fig. 3b.

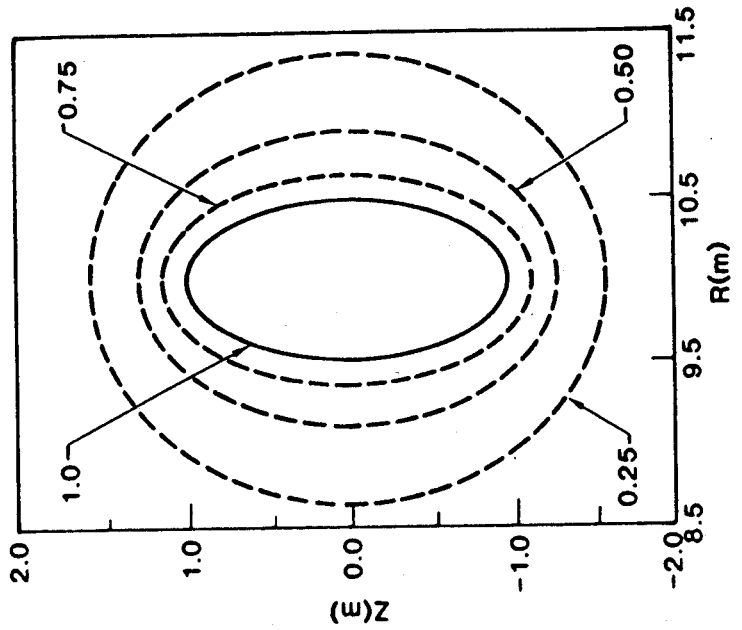

Haney and Freidberg, Fig. 4.

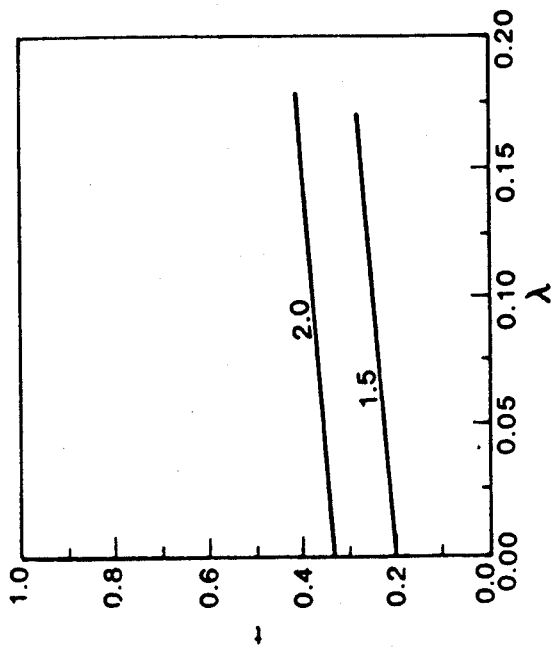

Haney and Freidberg, Fig. 5.

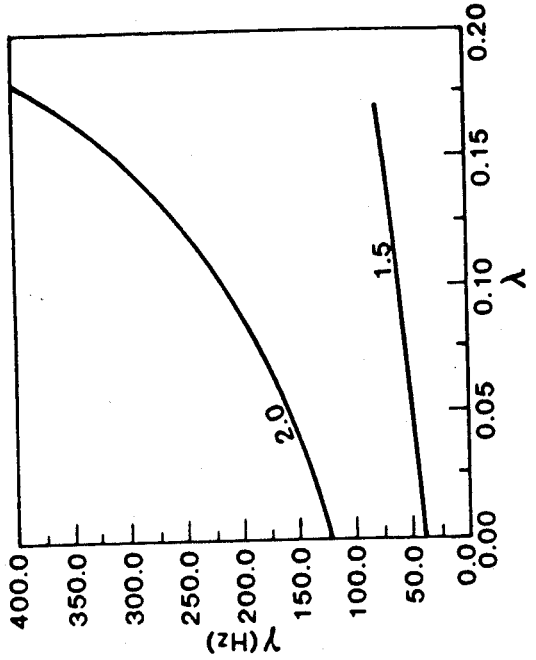

Haney and Freidberg, Fig. 6.